23rd ABCM International Congress of Mechanical Engineering
December 6-11, 2015, Rio de Janeiro, RJ, Brazil

LOCALLY REACTIVITY ANALYSIS OF MULTI CHAMBERS ACOUSTIC MUFFLERS USING MICROPERFORATED TUBES

Fernando H. Nardelli
Arcanjo Lenzi
UFSC – Federal University of Santa Catarina, Florianópolis, Santa Catarina, Brazil
e-mails fernando.nardelli@lva.ufsc.br, arcanjo.lenzi@ufsc.br

Abstract. *Dah-You Maa (1975) proposed a model for microperforated plates (MPP) panel absorber, with perforations reduced to submillimeter range and perforation ratio of about 1%. MPP provides satisfactory acoustic resistance, sufficiently low acoustic mass reactance, and substantial sound absorption. A muffler consisting of a microperforated tube backed by a number of cavities can be designed with Maa´s theory. Therefore, a simplified Finite Element Method (FEM) model could be used to represent this muffler, e.g. modeling microperforations and cavities with combined impedance, considering locally reactive cavities. If this assumption is not valid a more comprehensive FEM model is required. This model incorporates the main duct and the cavities applying a transfer admittance matrix to couple them. The aim of this research is to study the width of muffler cavities and understanding the behavior of local reactivity. The developed study is validated with Cremer optimum impedance theory, i.e. with an example of an optimized locally reactive filter.*

Keywords: *Microperforated Muffler, Transmission Loss.*

1. INTRODUCTION

The use of microperforations in acoustic filters is a recent development. These acoustic filters consist of a main perforated tube backed by cavities. This configuration results in great values of transmission loss in certain regions of the spectrum, if properly dimensioned. This phenomenon occurs due to the geometry potential of absorbing sound waves, which is provided by the damping effects of the holes. Note the difference with respect to a simple expansion chamber, where transmission loss is obtained by reactive effects.

Microperforated plates (MPP) theories were first developed by Maa (1975) in the context of panel absorbers. Thereafter, multiple authors developed researches regarding microperforated mufflers. For example, Kabral *et. al.* (2014) presented results of an optimization method based on the Cremer impedance, which provides the maximum absorption when applied in an infinite duct.

This paper aims to develop a FEM model for microperforated mufflers, revising Maa's microperforated theory, with an experimental validation. The final goal is to present an analysis of the locally reactivity of this kind of mufflers.

2. MPP IMPEDANCE MODELS

Microperforated plates are defined as plates with small perforations, around submillimeter, and porosity in the order of 1% (Maa, 1985). MPP provides high acoustic resistance and a negligible reactance. This configuration is suitable for panel absorbers, where the acoustic resistance must have values close to the impedance of the medium. Maa did his research considering only circular holed MPP. Nowadays his research was extended to slit-shaped MPP (Guo *et. al.*, 2008). Figure 01 depicts different kind of MPP. This research only consider circular holed MPP.

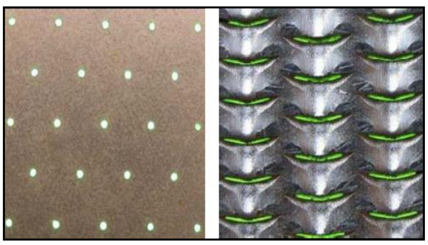

Figure 1. Circular holed (left) and slit-shaped holed (right) MPP, (Guo *et. al.*, 2008).

2.1 Circular Holed MPP Impedance

Starting with a single perforation that can be taken as a narrow tube, Maa (1985) defined a MPP as a plate with many circular holes, separated by a distance much larger than the diameter of the holes, but small if compared to the wavelength of the incident sound wave. Maa deduced the impedance of a single perforation based on the model of Rayleigh (1929) and Crandall´s (1926), and obtained the expression of the MPP impedance dividing the circular holes impedance by the porosity σ. Without end corrections, the MPP impedance can be expressed as:

$$Z = \frac{j\omega\rho t}{\sigma}\left[1 - \frac{2}{x\sqrt{-j}}\,\frac{J_1(x\sqrt{-j})}{J_0(x\sqrt{-j})}\right]^{-1}, \tag{1}$$

where $x = r_0\sqrt{\frac{\omega\rho}{\eta}}$, ρ is the fluid density, η is the dynamic viscosity coefficient, ω is the angular frequency, r_0 is the radius of the perforates and t is the plate thickness, while J_1 and J_0 are the first and zeroth Bessel functions, respectively. Note that x is inverse proportional to the relation between the perforation radius and the viscous boundary layer thickness, $\sqrt{\frac{2\eta}{\omega\rho}}$.

Equation 1 represents the effects inside the holes, not the outside effects. As the perforations diameter and the plate thickness are much smaller than the wavelength, the hole will behave as a piston. The movement of the fluid will push air around both sides of the perforation, attaching an additional mass. According to Crandall (1926) and Sivian (1935), the end correction δ is equal to $0{,}85d$, where d is the diameter of the hole, considering both sides of the hole. For a MPP this effect is given by

$$Z_{imag} = \frac{j0{,}85 d\omega\rho}{\sigma}. \tag{2}$$

Another effect is the power dissipation of an oscillating motion on a plane surface, which is given by $R_s = \frac{1}{2}\sqrt{2\eta\rho\omega}$ for an infinite plane, where η is the dynamic viscosity (Rayleigh, 1929). Based on experimental data Allam and Abom (2008) recommend the use of $4R_s$ for sharped edges holes and $2R_s$ for rounded edges holes. For a MPP, this term is determined by

$$Z_{real} = \frac{2\alpha R_s}{\sigma}, \tag{3}$$

where α is 2 for sharped edges holes and 1 for rounded edges holes.

2.2 Nonlinear and flow effects

Sivian (1935), Bolt et al. (1949), Ingard and Labate (1950) and Ingard (1953) were the authors to find the nonlinear effects on MPP. At high sound intensity, a jet is formed at the exit of the orifice, and as consequence of that the resistance increases with a corresponding increase in particle velocity. With this jet formation, acoustic energy is converted into vortices. Reactance decreases with the increase of particle velocity. This phenomenon occurs due to the fact that created vortices reduce the attached mass near the orifice. Maa (1994) presented the equations for the real and imaginary correction terms taking nonlinear effects into account. For flow effects, Allam and Abom (2008) and Ying et al (2008) proposed expressions where both effects can be represented separated for the real part of the impedance, but inside Z_{imag} for the imaginary part.

$$Z_{flow-real} = \frac{KM_g}{\sigma}, \tag{4}$$

where $K = 0.15\ \pm 0.0125$ and M_g is the Mach number of the grazing flow.

$$Z_{nonlinear-real} = \frac{\rho|u_h|}{\sigma}, \tag{5}$$

$$Z_{imag} = \frac{j0{,}85 d\omega\rho F(1+\frac{|u_h|}{\sigma c})^{-1}}{\sigma}, \tag{6}$$

where $F = \frac{1}{1+2.10^3.M_g{}^3}$.

2.3 Complete Impedance

Adding all corrections terms to the equation 1 of the MPP impedance one obtains:

$$Z = \frac{j\omega\rho t}{\sigma}\left[1 - \frac{2}{x\sqrt{-j}}\frac{J_1(x\sqrt{-j})}{J_0(x\sqrt{-j})}\right]^{-1} + \frac{2\alpha R_s}{\sigma} + \frac{KM_g}{\sigma} + \frac{\rho|u_h|}{\sigma} + \frac{j0{,}85d\omega\rho F(1+\frac{|u_h|}{\sigma c})^{-1}}{\sigma}. \tag{7}$$

3. CREMER IMPEDANCE OPTIMIZATION METHOD

Kabral *et. al.* (2014) presented an optimization method based on Cremer impedance. In 1953 Cremer derived an expression for the locally reacting impedance that provides maximum sound absorption when applied to infinite rectangular section ducts.

$$Z_{C-r} = \frac{(0.91-0.76j)\rho cka}{\pi}, \tag{8}$$

where k is wave number (m^{-1}) and a is the rectangular duct cross-section height (m).

In 1973 B. J. Tesler presented an expression for circular section ducts with mean flow.

$$Z_{C-r} = \frac{(0.88-0.76j)\rho ckr}{\pi(1+M_g)^2}, \tag{9}$$

where r is the circular duct radius (m).

This impedance represents the maximum achievable damping in the surface of an infinite duct, so if it was possible to achieve this impedance for each frequency, one could obtain the maximum transmission loss in a duct. Kabral *et. al.* applied this impedance to a finite duct, as shown in Fig. 02.

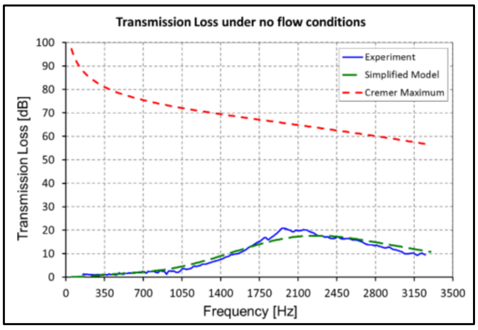

Figure 2. Transmission Loss of a model using Cremer Impedance (Kabral *et. al.*, 2014).

Kabral *et. al.* proposed to create a FEM model of a duct, applying the locally reacting impedance of the MPP combined to a locally reactive impedance for the cavities. The used cavity impedance was:

$$Z_{cav} = \frac{i\left[H_0^{(1)}(k_a r) - \frac{H_1^{(1)}(k_a R)}{H_1^{(2)}(k_a R)}H_0^{(2)}(k_a r)\right]}{H_1^{(1)}(k_a r) - \frac{H_1^{(1)}(k_a R)}{H_1^{(2)}(k_a R)}H_1^{(2)}(k_a r)} \tag{10}$$

where k_a is the axial wave number (m^{-1}), R is the radius of the expansion chamber (m), r is the radius of main duct (m), and $H_m^{(n)}$ is the Hankel function of n:th kind and m:th order. In a locally reactive surface the effects are the same in all the points, which means that one point doesn't affect the others. On the cavity impedance (Eq. 10), for example, only radial effects are represented, which means that the locally reactive model does not predict axial sound wave propagation.

For the optimization, the authors carefully chose the geometric properties of the MPP and the cavity radius to adjust the impedance of the model according to Cremer impedance to 2000 Hz. First, it was found a MPP configuration that fits the real part of Cremer Impedance. Second, the imaginary part was set, combining the MPP with the cavity impedances. The result for the transmission loss (TL) analysis is showed in Fig. 3. As expected, the TL result of the optimized model coincides with the Cremer model at the chosen fitted frequency.

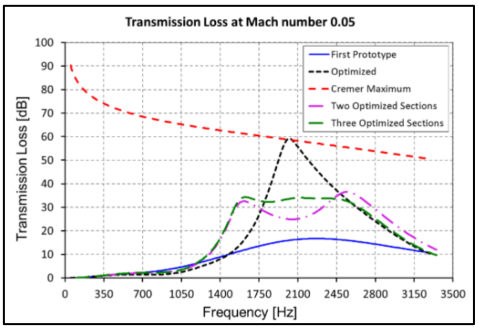

Figure 3. Transmission Loss of a model optimized for 2 kHz (Kabral *et. al.*, 2014).

4. NUMERICAL MODEL

A non-locally reactive numerical model is proposed in this application. The cavities are modeled by FEM and the MPP is represented by a transfer admittance matrix that connects the main duct mesh with the cavities mesh. This matrix is defined using the MPP impedance, as described on section 2.3. The model is developed in the commercial software *LMS Virtual.Lab,* as depicted in Fig. 4. The transfer admittance matrix is:

$$\begin{bmatrix} v_{n1} \\ v_{n2} \end{bmatrix} = \begin{bmatrix} A_p & -A_p \\ -A_p & A_p \end{bmatrix} \begin{bmatrix} p_1 \\ p_2 \end{bmatrix}, \tag{11}$$

where v_{n1} and v_{n2} are the velocities in surfaces 1 and 2, p_1 and p_2 are the pressures in surfaces 1 and 2 and $A_p = \frac{1}{Z_{MPP}}$. In this model, all the effects that might occur in the cavities are calculated by the FEM solver.

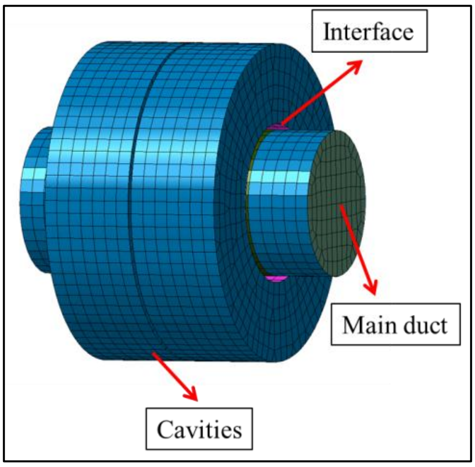

Figure 4. Mesh of the numerical model. The main duct and the cavities are connected with the transfer admittance matrix.

5. EXPERIMENTAL VALIDATION

For the experimental validation an impedance tube was built according to the ASTM E2611-09 Standard, except for the material, since acrylic plastic was used instead of steel. The tube was designed for measurements in a frequency range of 120 Hz to 4300 Hz. Figure 6 depicts the impedance tube.

Figure 6. Impedance tube for transmission loss measure.

Tests have been conducted to evaluate the quality of the impedance tube, by measuring a simple expansion chamber. The maximum variation found between the measurement and a numerical analysis was less than 2 dB in transmission loss. The chosen measurement was the two load method, described in the standard.

To validate the numerical model, a MPP muffler was built, as depicted in Fig. 7. Figure 8 shows a schematic for the muffler. The properties of the muffler were set using the optimization method described in section 3.

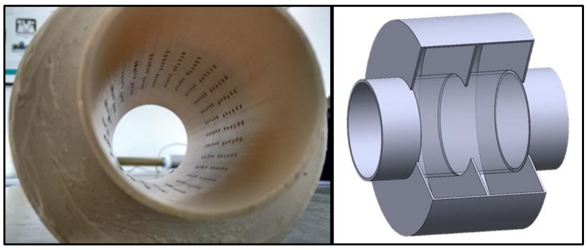

Figure 7. MPP Muffler prototype.

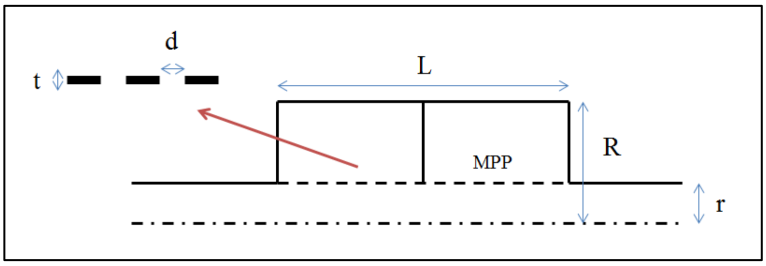

Figure 8. Schematic of the prototype.

where: t = 2 mm, d = 1,5 mm, L = 56 mm, R = 50 mm, r = 23 mm and σ = 6,667 %.

Results are shown in Fig. 9. For this model flow and nonlinear effects were not considered.

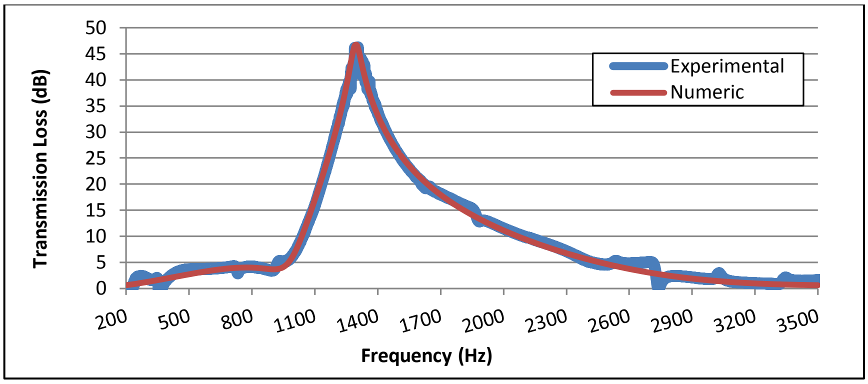

Figure 9. Transmission loss for the numeric and experimental analisys.

It can be seen that the proposed numeric model is correspondent to the real model.

6. LOCALLY REACTING ANALYSIS

With the validated model, a locally reacting analysis was made. This analysis consists of an optimized model, based on Cremer Impedance, using Kabral *et. al.* method. Thereafter, non-locally reactive models were made and simulated, increasing the number of cavities, but with the same MPP region. The length of the cavities are set in relation with the wavelength of the locally reactive TL peak. The properties of the MPP muffler are the same as used in the validated model, except for the total length, which is set to 300 mm. As the peak frequency of locally reacting model is 1130 Hz, and the sound speed is 340 m/s, the wavelength is very close to 300 mm.

The models showed in Tab. 1 were simulated and the results for the transmission loss are depicted in Fig. 10.

Table 1 – Analyzed models.

Number of cavities	Length of each cavity (mm)
01	300
02	150
04	75
06	50
12	25
20	15
30	10

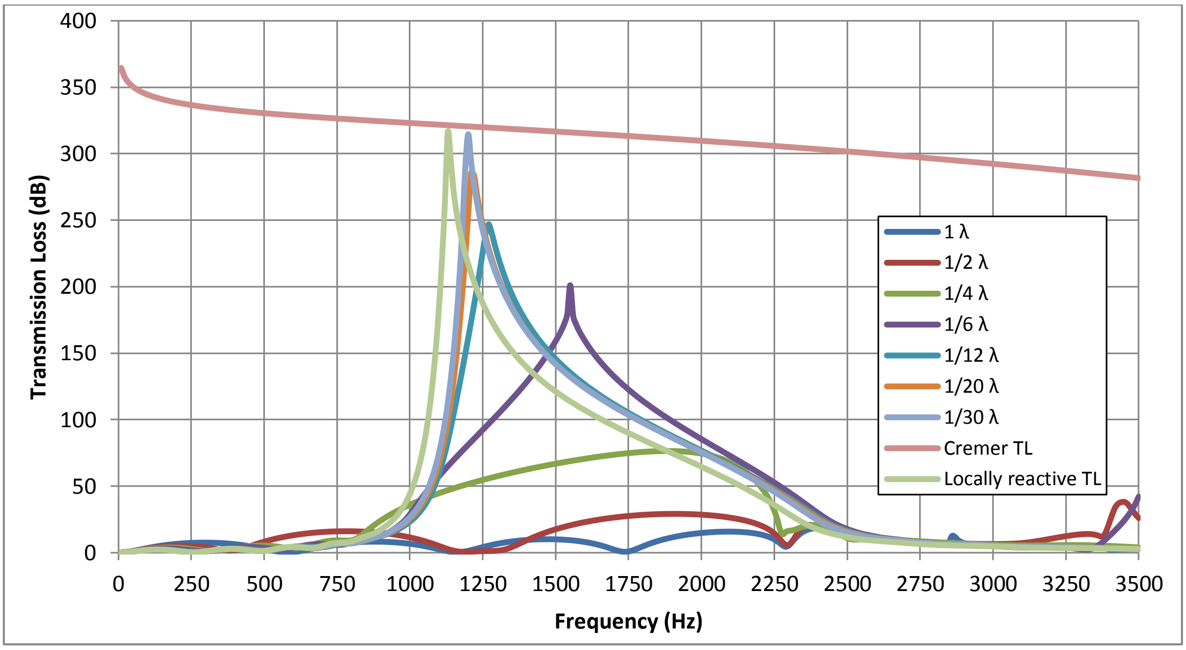

Figure 10. Transmission Loss for the analyzed configurations.

It can be seen that by increasing the number of cavities the peak frequency approaches the locally reactive model results, but even with *λ/30* cavity length the model still is not locally reactive. Figures 11 and 12 show the difference between the locally reactive model and the non-locally reactive analysis.

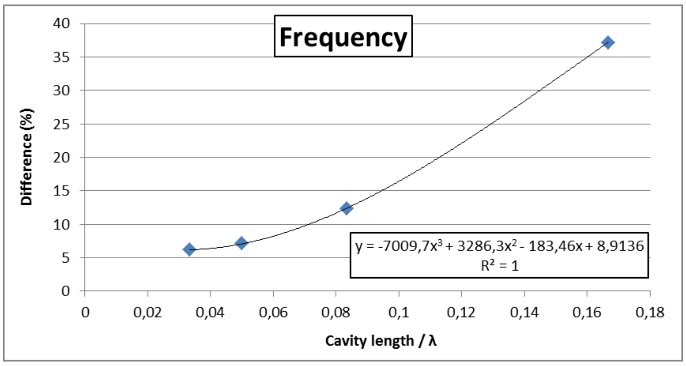

Figure 11. Relation between peak frequency and cavities length, in comparison with the locally reactive model.

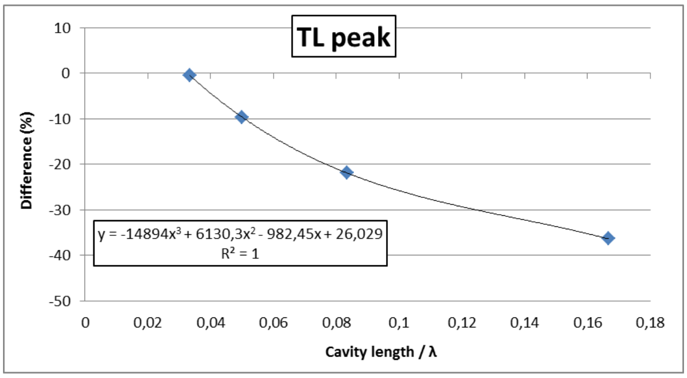

Figure 12. Relation between TL peak and cavities length, in comparison with the locally reactive model.

With this information one can estimate the peak frequency of a non-locally reactive model, with the correspondent locally reactive model and the length of the cavities. Note that there is a perfect third order fit in Frequency and TL peak.

7. CONCLUSIONS

MPP applied into acoustic mufflers have the potential to provide great levels of TL in some bandwidth. Using different configurations on each chamber of a multi chamber muffler makes possible to achieve a more distributed TL curve, with considerable levels of transmission loss. The validated prototype achieved almost 50 dB of transmission loss without large dimensions, which shows the great potential of this kind of muffler.

Maa's theory showed great correspondence with the tested model, even with larger porosity and diameter of holes.

To estimate the transmission loss of a muffler using numeric analysis a locally reactive model can be used, but is important to note that it will appear a difference in the peak frequency and level of transmission loss, which will decrease by decreasing the width of the chambers, as showed in this paper.

8. REFERENCES

1. Allam, S. and Abom, M., "Experimental characterization of acoustic liners with extended reaction", 14th AIAA/CEAS Conference, 2008.
2. Bolt, R. H., Labate, S., and Ingard, U., "The acoustic reactance of small circular orifices", J. Acoust. Soc. Am., 21, 94-97, 1949.
3. Crandall, I. B., "Theory of vibration system and sound", Van Nostrand, New York, p. 229, 1926.
4. Guo, Y., Allam, S., and Abom, M., "Micro-perforated plates for vehicle application", INTER-NOISE 2008, Shangai, China, 2008.
5. Ingard, U., and Labate, S., "Acoustic circulation effects and the nonlinear impedance of orifices", J. Acoust. Soc. Am., 22, 211-219, 1950.
6. Ingard, U., "On the theory and design of acoustic resonators", J. Acoust. Soc. Am., 25, 1037-1062, 1953.
7. Kabral, R., Du, L., Abom, M., and Knutsson, M., "A compact silencer for the control of compressor noise", SAE Int. J. Engines 7(3), 1572-1578, 2014.
8. Maa, D.-Y., "Theory and Design of microperforated panel sound absorbing construction", Sci. Sin. XVIII, 55-71, 1975.
9. Maa, D.-Y., "Microperforated-Panel wideband absorbers", Institute of Acoustics, Academia Sinica, China, 1985.
10. Maa, D.-Y., "Microperforated panel at high sound intensity", Proceedings of Internoise 94, Yokohama, Japan, 1994.
11. Rayleigh, L., "Theory of Sound II", MacMillan, Ney York, p. 327, 1929.
12. Sivian, L. J., "Acoustic impedance of small orifices", J. Acoust. Soc. Am., 7, 94-101, 1935.

9. RESPONSIBILITY NOTICE

The authors are the only responsible for the printed material included in this paper.